Deep-Sea Research II 57 (2010) 508–518

Contents lists available at ScienceDirect

Deep-Sea Research II

journal homepage: www.elsevier.com/locate/dsr2

Three-dimensional observations of swarms of Antarctic krill (*Euphausia superba*) made using a multi-beam echosounder

Martin J. Cox [a,*], Joseph D. Warren [b], David A. Demer [c], George R. Cutter [c], Andrew S. Brierley [a]

[a] Pelagic Ecology Research Group, Gatty Marine Laboratory, University of St. Andrews, Fife KY16 8LB, Scotland, UK
[b] School of Marine and Atmospheric Sciences, Stony Brook University, 239 Montauk Hwy, Southampton, NY 11968, USA
[c] Advanced Survey Technology Program, Southwest Fisheries Science Center, 8604 La Jolla Shores Drive, La Jolla, CA 92037, USA

ARTICLE INFO

Article history:
Accepted 30 October 2009
Available online 11 November 2009

Topical issue on "Krill Biology and Ecology." The issue is compiled and guest-edited by the North Pacific Marine Science Organization (PICES), International Council for the Exploration of the Sea (ICES), and Global Ocean Ecosystem Dynamics (GLOBEC) project.

Keywords:
Antarctic krill
Euphausia superba
Pelagic
Multibeam echosounder
Swarm morphology
Three dimensions
Livingston Island
South Shetland Islands

ABSTRACT

Antarctic krill (*Euphausia superba*) aggregate in dense swarms. Previous investigations of krill swarms have used conventional single- or split-beam echosounders that, with post-processing, provide a two-dimensional (2-D) view of the water column, leaving the third dimension to be inferred. We used a multi-beam echosounder system (SM20, 200 kHz, Kongsberg Mesotech Ltd, Canada) from an inflatable boat (length=5.5 m) to sample water-column backscatter, particularly krill swarms, directly in 2-D and, with post-processing, to provide a three dimensional (3-D) view of entire krill swarms. The study took place over six days (2–8 February 2006) in the vicinity of Livingston Island, South Shetland Islands, Antarctica (62.4°S, 60.7°W). An automatic 3-D aggregation detection algorithm resolved 1006 krill swarms from the survey data. Principal component analyses indicated that swarm morphology metrics such as length, surface area and volume accounted for the largest between swarm variance, followed by echo energy, and finally swarm geographic location. Swarms did not form basic cylindrical or spherical shapes, but had quite consistent surface area to volume ratios of 3.3 m^{-1}. Swarms were spatially segregated, with larger sizes (mean north-south length=276 m, at least double that of two other swarm classifications), found to the northwest of the survey area. The apparent clustering of swarm types suggests that krill biomass surveys and ecosystem investigations may require stratified survey design, in response to varying 3-D swarm morphology, variation that may be driven in turn by environmental characteristics such as bathymetry.

1. Introduction

Many pelagic marine organisms exhibit patchy spatial distributions that are driven by a variety of biotic and abiotic factors (Genin, 2004). Aggregation appears to be a fundamental component of the behaviour of Antarctic krill (*Euphausia superba*), and indeed the swarm has been referred to as the "fundamental unit of krill ecology" (Murphy et al., 1988; Hofmann et al., 2004). Aggregations of Antarctic krill may form as a consequence of individuals seeking to reduce the chance of predation (O'Brien, 1987; Hamner and Hamner, 2000; Szulkin and Dawidowicz, 2006), to facilitate mating and/or feeding (Watkins et al., 1992; Miller et al., 1993; Hofmann et al., 2004), or to convey locomotive energetic advantage (Ritz, 1994, 2000).

Previous investigations suggest there are large variations in krill swarm shape (Miller et al., 1993; Woodd-Walker et al., 2003) and packing density (Barange et al., 1993). Swarm dimensions and density have been used to classify swarms into types, and previous studies have implied spatial clustering of swarms by type (Miller and Hampton, 1989; Watkins and Murray, 1998). For example, Mauchline (1980) classified three types of aggregation based on numerical density: the densest swarm type contained from 1000 to 100,000 krill m^{-3}; and was followed by logarithmically decreasing class densities of 1 to 100 and 0.1 to 1 krill m^{-3}.

It is believed that some of the observed variation in swarm density and shape occurs in response to environmental conditions (Barange et al., 1993; Alonzo and Mangel, 2001; Hofmann et al., 2004), such as upwelling or localised water currents that occur in the vicinity of rapid changes in bathymetry (Trathan et al., 2003). It will be important to understand how krill aggregate to elucidate possible relationships between various potential physical or biological forcing mechanisms and swarm shape. This in turn would enable the extent to which krill demographics (e.g., age, sex, and maturity) are important to swarm formation (Watkins et al., 1986, 1992; Tarling et al., 2007). Understanding the mechanisms of krill swarm formation, and potential spatial variation in these mechanisms, may also be vital for unbiased

* Corresponding author. Tel.: +44 1334 463457; fax: +44 1334 463443.
E-mail address: mjc16@st-and.ac.uk (M.J. Cox).

0967-0645/$ - see front matter © 2009 Elsevier Ltd. All rights reserved.
doi:10.1016/j.dsr2.2009.10.003

estimates of biomass (Gerlotto et al., 1999), and for addressing ecological issues such as predator–prey interactions (Zamon et al., 1996) and responses by krill to variation in their abiotic environment such as water depth (Hewitt and Demer, 2000; Trathan et al., 2003).

Most observations of krill swarms have been made acoustically with scientific echosounders, as per biomass surveys (e.g., Everson and Miller, 1994). Acoustic observations of krill swarms made using conventional vertically-downward looking single- or split-beam echosounders (SBE) are limited by the small conical sampling volumes (typically 7°) inherent with these instruments. Following each SBE acoustic transmission (ping), samples of volume backscattering strength (S_v) are recorded versus sound-propagation time, or water depth. Sequential recordings combine to build up a two-dimensional (2-D) matrix of water-column observations (Reid and Simmonds, 1993). The narrow acoustic beam effectively samples only a 2-D slice through the water column and any krill swarm in it. The three-dimensional (3-D) krill swarm shape cannot be estimated directly from 2-D observations without making assumptions about the swarm shape (e.g., it is cylindrical or spherical; Simmonds and MacLennan, 2005). Consequently, the volume of a krill swarm that falls outside of the narrow SBE beam cannot be determined. Krill biomass estimation techniques and investigations into krill ecology would both benefit from improved 3-D observations of individual krill swarms.

In this investigation, we used a multi-beam echosounder system (MBE) to observe Antarctic krill swarms in 2-D in the field, and extended these 2-D MBE observations into 3-D visualisations of swarms during post-processing. The purpose of this investigation was three fold. Firstly we sought to determine if krill could be observed in the nearshore environment using an MBE deployed from a small boat. Secondly, we wanted to investigate if the 3-D acoustic reconstruction of krill swarms could be used to improve understanding of the variability of swarm shape and density. Thirdly, we sought, using multivariate analyses, to examine the scale of variation of various swarm metrics. We hoped that, if successful, combining these elements could lead to future incorporation of MBEs into studies to improve understanding of krill biology and ecology.

2. Materials and methods

Two inflatable boats (Mark V Zodiacs, length=5.5 m) were deployed in the vicinity of Cape Sheriff, from 2 to 9 February, 2006. Operational constraints meant that a different number of transects was sampled each day (Fig. 1). The survey-site seabed depth ranged from 20 to 140 m. Seabed depth is an important consideration because it influences the MBE sampling volume and, due to side-lobe interference, the maximum observable across-track swarm width.

One inflatable boat, R/V *Roald*, was equipped with an MBE (200 kHz SM20, Kongsberg Mesotech Ltd, Canada) and conducted a high-resolution seabed-bathymetry survey (100% seabed coverage, resolution=1 m) with simultaneous water-column sampling to observe krill swarms acoustically. The second inflatable boat, R/V *Ernest*, was equipped with 38 and 200 kHz SBEs (calibrated single-beam Simrad ES60s). The MBE survey comprised 35 2.5-km transects and four 3.5-km transects, each with a 120 m inter-transect spacing (Fig. 1). On the final day of surveying, two 'tie lines' of length=5.2 km with spacing=1.2 km were run perpendicular to the main transects, the purpose of which was to assess any day affect (i.e. possible day-to-day variation) in the MBE krill swarm data. In addition to acoustic observations, visual observations of air-breathing krill predators were collected from both Zodiacs (Cox et al., 2009).

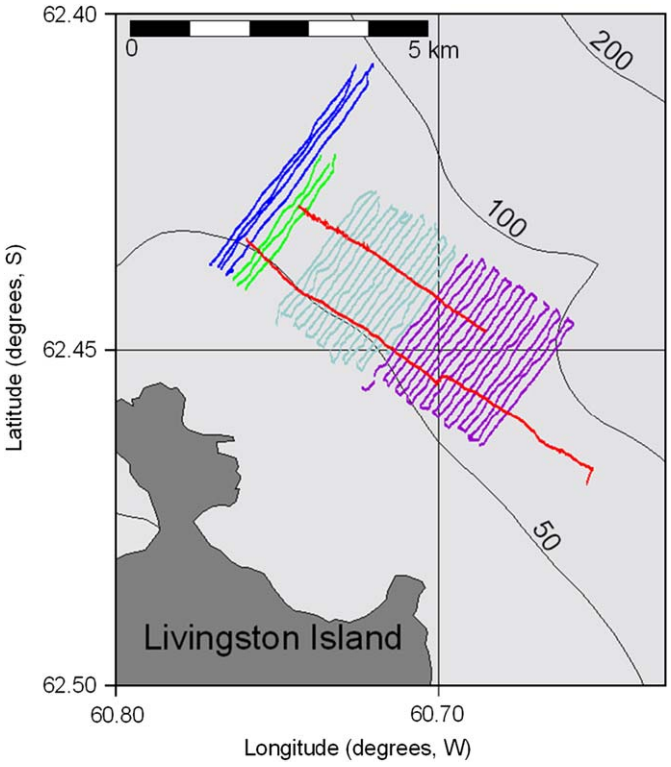

Fig. 1. The Cape Sheriff study site, Livingston Island, South Shetlands, Antarctica. Multi-beam survey transects are shown, colour coded by day. Bathymetric contours are shown as black lines. Note the two tie-lines which were surveyed perpendicular to the main survey.

2.1. Multibeam equipment and data description

The MBE had a total swath width of 120°, made up of 128 receive beams each with a 1.5° across-track and 20° along-track beam width. The MBE head was mounted facing vertically downwards, along the centreline of the boat, so ensonified a 60° swath either side of the track line. An orthogonally-mounted (with respect to the MBE head) external profiling transmitter was used and reduced the along-track beam width from 20° to 1.5°. This improved the precision of water-column target sampling and reduced between-ping along-track sampling volume overlap. Acoustic pulses were transmitted every 1.5 to 3 s (this varied because of computer processing limitations). Time varied gain was $20\ log_{10}(range)$, pulse length was 825 μs, and the transmission power was set to 'medium'. MBE detections throughout the fixed 200-m observation range had 0.5 m resolution to standardise sampling and were logged continuously to the control computer. Recorded MBE data were converted to the SM2000 data format using Kongsberg Mesotech MsToSm (v1.0), and resulting S_v data were processed using Echoview v3.5 (Myriax, Hobart, Australia).

2.2. Scaling uncalibrated MBE S_v observations

The MBE cannot be calibrated easily in the field using the conventional standard reference sphere techniques (Foote et al., 1987) that would typically be applied to SBEs. Consequently, the uncalibrated data from the MBE were calibrated by comparison to the S_v observations calibrated by the standard sphere method and collected by the ES60 along the tie lines (two lines run

perpendicularly to the 41 main MBE survey transects, Fig. 1). The tie lines were surveyed with the SBE-equipped R/V *Ernest* following the MBE-equipped R/V *Roald*. The Zodiacs were separated by approximately 200 m to avoid acoustic cross-talk between the 200 kHz systems, but essentially sampled the same bodies of water. Thus, it was assumed that both instruments sampled the same distribution of water-column backscatter.

The S_v data from the SBE and the nadir beam (number 63) of the MBE were compared. Krill swarm boundaries were determined using the SHAPES algorithm implemented in the Echoview schools detection module (see Barange, 1994; Coetzee, 2000). Then, the data were spatially aligned and averaged in 2 ping by 3 m vertical cells. Echoes from krill were identified in the gridded SBE data using the dB difference technique (Brierley et al., 1998; $-0.7 < S_{v\_200\ kHz} - S_{v\_38\ kHz} < 13.3$ dB). Gridded mean S_v values from both instruments for grid cells lying within the SBE detected swarms were used to determine the cumulative density functions (CDFs) for the mean S_v from both the SBE (CDF_{SBE}) and the MBE (CDF_{MBE}). Both CDFs were calculated using

$$p(t) = (1/n)\sum_{i=1}^{n} I(x_i)$$

where $I(x_i)$ is an indexing function:

$$I(x_i) = \begin{cases} 1 & : \ x_i \le t \\ 0 & : \ \text{otherwise} \end{cases}$$

t is the required resolution for the CDF mapping, i is S_v observation number and n is the total number of S_v observations. The two CDFs were mapped by determining which gridded S_v values from both acoustic instruments occurred at equal proportions $p(t)$ along their respective CDFs (left panel, Fig. 2). This between-instrument map was used as a look-up table to rescale the MBE S_v observations to equivalent ES60 S_v.

2.3. Automated 3-D krill swarm detection and sensitivity analysis

Krill swarms were identified from the MBE observations using a 3-D school detection algorithm (Echoview v 3.5 multibeam module, Myriax). The algorithm identifies contiguous groups of acoustic returns in each beam and bounds with prisms the extremities of each acoustic return group. These prisms are triangulated, reducing each prism to two triangles. The perimeter of the 3-D school is generated by retaining the visible vertices of the triangles, which are used to create a 3-D bounding surface around the contiguous acoustic return. At this point, the user-defined size parameters, minimum longest dimension, minimum middle dimension and minimum shortest dimension, are used to eliminate detected swarms with dimensions smaller than these minimum parameters. In addition, the minimum S_v threshold (dB re m^{-1}, S_{v_t}) defines the minimum density of acoustic returns that are transferred to the 3-D detection algorithm, hence defining the krill swarm boundary. Acoustic observations of ranges less than 5 m were ignored due to sea-surface noise and near-field effects (Melvin et al., 2003). For the purposes of 3-D target detection, the search volume for the 3-D algorithm was constrained to water column targets by referencing 0.5 m above the seabed as defined by the MBE sounder detected bottom identification algorithm. For each identified swarm, various metrics were extracted (see Table 1 for description of quantitative swarm descriptor variables).

The sensitivity of perceived swarm metrics (Table 1, shown in italics) to variation of the 3-D detection algorithm parameters was investigated (Table 2) and used to select an optimum set of parameters as follows.

Four transects, (numbers 2, 17, 22 and 33), were selected at random from the total of 41 transects run to furnish data for the sensitivity analysis. The sensitivity of the 3-D school detection parameters was investigated in two stages. Firstly, the three minimum dimension parameters (minimum longest, middle and

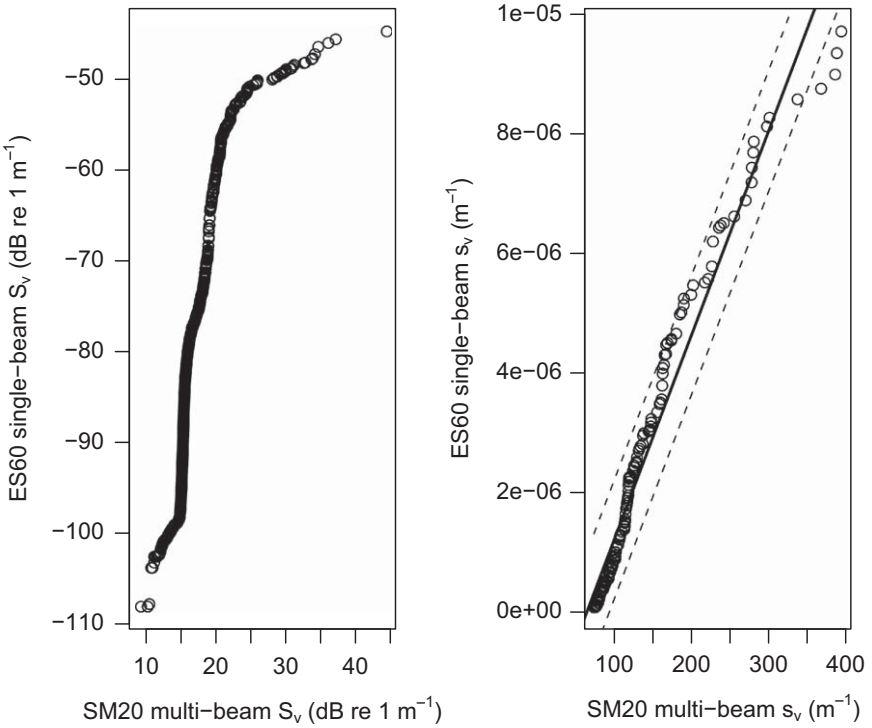

Fig. 2. SM20 calibration. Left panel: The cumulative distribution function (CDF) mapping of the uncalibrated SM20 multi-beam echosounder S_v observations and calibrated ES60 single-beam echosounder S_v observations (Section 2.2). Right panel: The linear relationship between the CDF of the SM20 and ES60 in the linear domain (s_v). The CDF linear relationship occurs in the range -70 dB < ES60 S_v < -50 dB. The linear regression (r^2_{adj}=0.96, $p < 2.2e^{-16}$, black line) and 95% prediction intervals (dotted black line) are shown.

Table 1
Krill swarm metrics used in multi-variate analysis. Metrics used in the 3-D detection algorithm sensitivity analysis shown in italics (Section 2.3).

Metric name	Abbreviation	Units	Description
Surface area	S	m^2	Surface area of the 3-D krill swarm
North-south length	l_{NS}	m	Maximum length of the 3-D swarm along a north-south
East-west length	l_{EW}	m	Maximum length of the 3-D swarm along a east-west
Height	h	m	Maximum swarm height (z_{max}–z_{min}). z_{max}=maximum swarm depth, z_{min}=minimum swarm depth.
Volume	V	m^3	3-D swarm volume
Roughness	R	m^{-1}	$R=S/V$
Length/height ratio	l/h	–	length/height
S_{v_mean}	S_v	dB re 1 m^{-1}	Mean volume backscattering strength within a swarm
S_{v_min}	S_{v_min}	dB re 1 m^{-1}	Minimum S_v
S_{v_max}	S_{v_max}	dB re 1 m^{-1}	Maximum S_v
Seabed depth under swarm[a]	z	m	Seabed depth under geometric centre of swarm
Position in water column[a]	$posn_{wc}$	–	$posn_{wc}=1-(\lvert z_{max}-z\rvert/z)$ giving $0<posn_{wc}<1$
geometric centre position	(ϕ, λ)	deg	Latitude and longitude of geometric centre of 3-D krill swarm.
geometric centre depth	Z	m	Depth at the geometric centre of the 3-D krill swarm.
Nearest neighbour distance	NND	m	Radial distance calculated using great circle distance
Time of day (GMT)	t		Time of swarm observation
Cross track distance[a]	x	m	Cross track distance from geometric centre of swarm to MBE

[a] Not calculated using Echoview.

Table 2
Parameters used in the SonarData 3-D detection algorithm and values used during the sensitivity analysis (Sections 2.3 and 3.1).

3-D schools detection parameter	Units	Parameter values used in sensitivity analysis
Minimum longest, middle and shortest dimensions	m	2, 3, 4, 5, 6, 10, 15, 30 and 35
Minimum mean volume backscatter threshold (S_{v_t})	dB re 1 m^{-1}	19 to 29 in 1 dB re 1 m^{-1} increments

shortest aggregation dimensions) were varied. In the absence of any prior information about the 3-D shape of krill swarms in the nearshore study region, the same length was used for each of the 3-D detection length parameters (Table 2), with the minimum MBE detection threshold fixed at $S_v=-51.8$ dB re 1 m^{-1} or approximately 166 krill m^{-3} using a TS=−74 dB re m^2). The second part of the sensitivity analysis investigated the effect of varying the minimum threshold, with the minimum school dimensions set to 5 m.

2.4. 3-D krill swarm descriptors

The 2-D nearest-neighbour-distance (NND) was calculated using the great circle distance between the geocentric latitude and longitude of each detected krill swarm (Table 1). To determine the krill swarm metrics that accounted for the largest inter-swarm differences, a principal component analysis (PCA) was performed. Because some of the 3-D swarm metrics had different units and scales (e.g., swarm geometric latitude and swarm volume) the PCA was carried out on a matrix of normalised krill swarm metrics. To aid interpretation of the PCA eigen vectors, individual eigen vector elements (u_{ij}) greater than a scaling factor $|u_{ij}|>0.7.\max(|u_j|)$ (Mardia et al., 1979) was used to identify which swarm metrics exerted more influence on individual principal components than average, and thus made the greatest contribution to inter-swarm variation. A three-type partition analysis was then performed in the reduced factorial space provided by the PCA results to determine if swarms formed distinct types. A three-type partition was selected based on the classification schemes of Mauchline (1980). The appropriateness of the three-type analysis was validated by the results of a pseudo F-test for analyses with different numbers of clusters (Johnson, 1998), that determined differences in the sums of squares of within cluster differences.

3. Results

Using 'optimal' detection parameters (see Sections 2.3 and 3.1), a total of 1084 krill swarms were observed using the MBE, of which 1006 were determined to be entirely within the MBE sampling volume (i.e. not extending into side lobes or beyond the outermost beams).

3.1. 3-D detection algorithm sensitivity analysis

Sensitivity analysis of the minimum school dimension showed that the number of detected swarms decreased with increasing minimum swarm dimensions (Fig. 3). Median swarm height, north-south and east-west length, and swarm volume all increased with increasing minimum swarm dimensions. Median minimum NND increased with increasing minimum swarm size, partly since fewer swarms were detected. The NND results at larger minimum swarm sizes indicated that the few remaining large, high-density ($S_v>S_{v_t}$) krill swarms were not spatially clustered.

While the sensitivity plots (Fig. 3) were informative, there was insufficient information to determine analytically the minimum dimension swarm detection parameters. Visual inspection of the 3-D krill swarm boundaries generated using the detection algorithm showed that the 2-m minimum school dimension (Table 2) caused splits in larger swarms and an increase in the number of seabed side-lobe detections being identified spuriously as aggregations. It was not possible to remove seabed side-lobe detections prior to running the 3-D detection algorithm because the side-lobe detections varied from ping-to-ping. The 5-m minimum school dimension reduced spurious identification of side lobes and prevented spurious identification of krill swarm boundaries, but did occasionally split krill swarms. The 10-m minimum length setting degraded the detected krill swarm spatial resolution and eliminated small swarms. This degradation of krill swarm spatial structure and elimination of smaller krill swarms persisted with increasing minimum 3-D length settings.

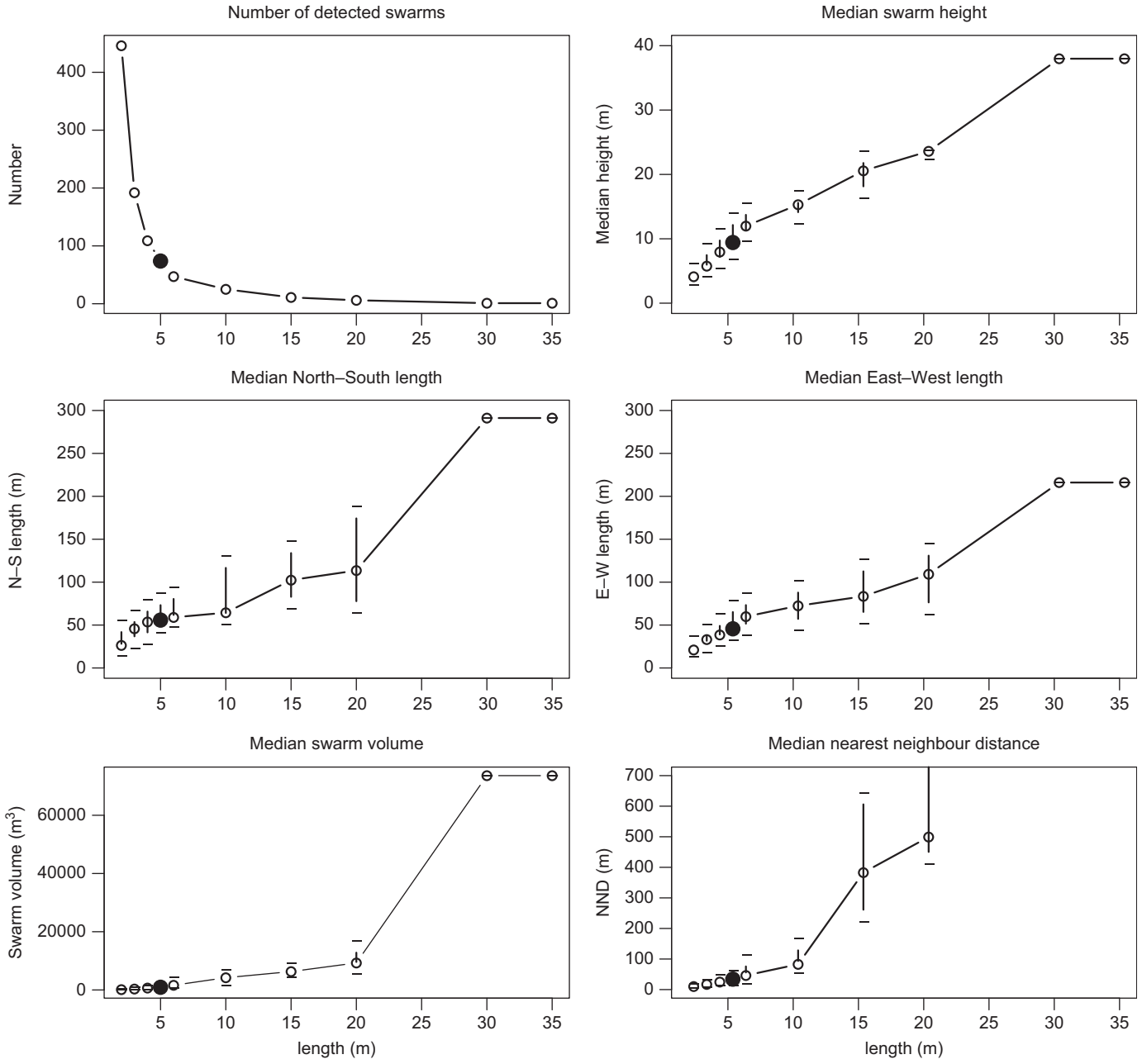

Fig. 3. Sensitivity of krill swarm descriptive metrics (Median, 25% and 75% quantiles shown) to the minimum 3-D school size detection parameters, with the selected school size parameters (5 m) shown as black circles. Minimum threshold, S_{v_t}, was set to 23 dB re 1 m^{-1} throughout the analysis.

Consequently the 5-m minimum length setting was selected as a compromise.

A sensitivity analysis of processing threshold $S_{v_t} < -67.6$ dB re 1 m^{-1} (ca. 5 animals m^{-3}) was not used because the number of background noise detections prevented the 3-D school detection algorithm from functioning correctly at low processing thresholds. The relationships between number of detected swarms and S_{v_t} showed that more swarms were detected at lower S_{v_t} (Fig. 4). The maximum median swarm height and volume occurred when the $S_{v_t} = -52.7$ dB re 1 m^{-1} (ca. 133 animals m^{-3}). At lower S_{v_t}, the 3-D detection metrics contain data from side lobe and noise detections that generally result in 3-D detections with smaller volumes than those attributed to 3-D krill swarm detections. At $S_{v_t} > -52.7$ dB re 1 m^{-1}, the lower density edges of detected krill swarms were eroded, resulting in reductions in all median krill swarm metrics. Given that at $S_{v_t} = -57.7$ dB re 1 m^{-1} maximum swarm height and volume occurred, and the number of spurious side lobe detections fell, this was selected as the S_{v_t} for 3-D schools detection of krill swarms. Therefore, for the purposes of this investigation, a krill swarm is defined as a collection of acoustic samples with $S_{v_t} > -57.7$ dB re 1 m^{-1} with spherical dimensions > 5 m. Using these 3-D detection parameters, a conventional vertically-downward looking SBE with a 7° beam would not sample an entire spherical krill swarm with a 5 m diameter until a depth of 57 m. Only 52% of MBE detected swarms were found deeper than 57 m, which illustrates the constraints prevalent with SBE: swarms of the 5-m example diameter cannot be entirely sampled with an SBE until a depth of at least 57 m. Despite the external envelope of swarms being defined using 3-D schools detection parameters of 5 m for shape and $S_{v_t} = -57.7$ dB

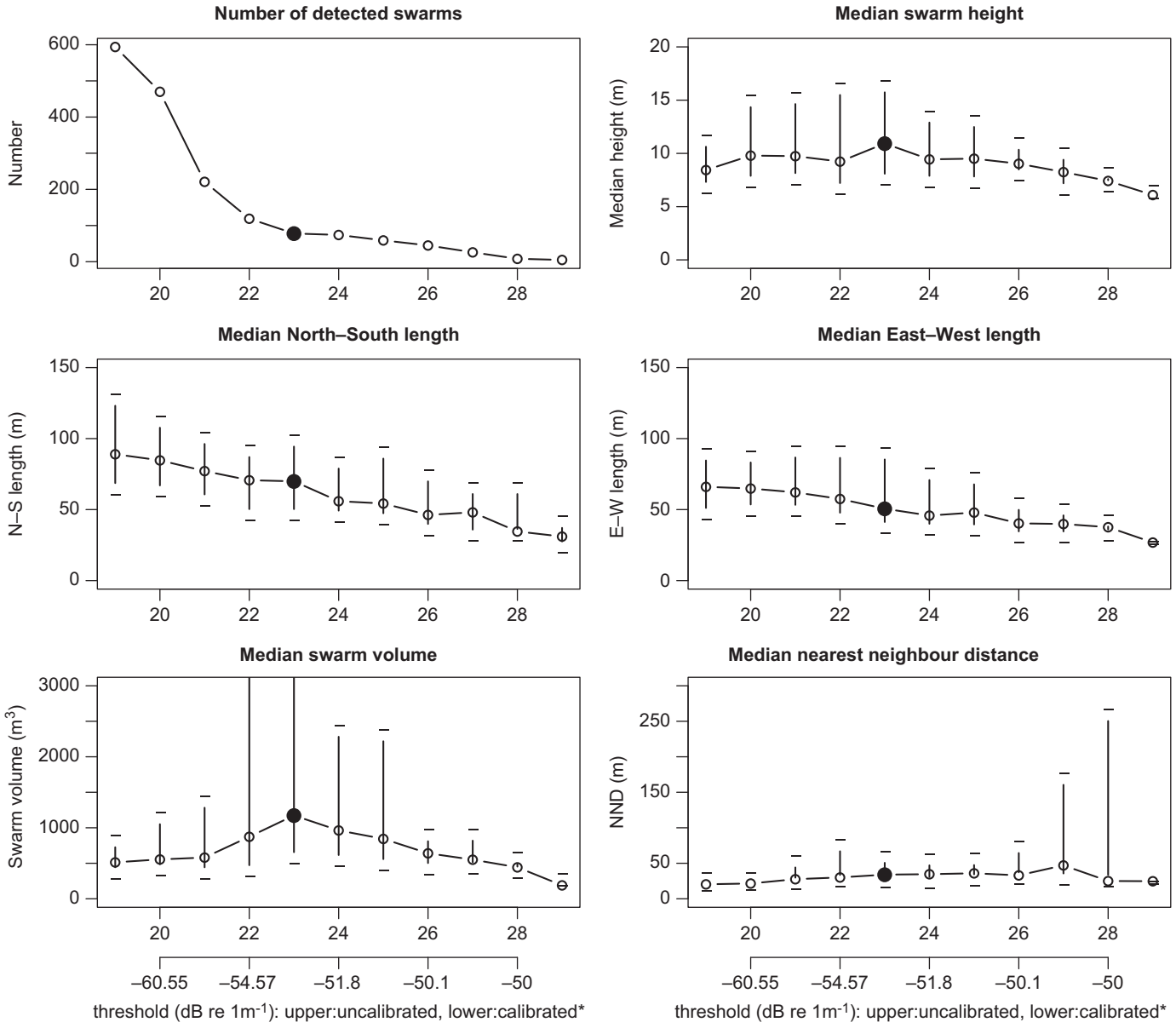

Fig. 4. Sensitivity of krill swarm descriptive metrics to variations in the minimum detection threshold (S_{v_t}). Points are median metric values with 25% and 75% quantiles. The selected S_{v_t}=23 dB re 1 m^{-1} is shown as black circles. *X*-axis scale is given in uncalibrated MBE S_v (upper-scale) and ECDF mapped, approach one, MBE S_v (lower-scale). Note *Method 1 calibration by comparison used (see Section 2.2). The 75% quantile for median swarm volume is 3,311 m^3 at S_{v_t}=23 dB re 1 m^{-1} and 3,421 m^3 at S_{v_t}=24 dB re 1 m^{-1}.

re 1 m^{-1}, the S_{v_t} was removed when analysing the observations within the 3-D swarm boundary. This means the energetic measures of swarms are essentially unthresholded values.

3.2. Krill swarm morphology

As an initial investigation of swarm morphological types, the ratio of swarm length to height (*l*/*h*) was calculated. A continuous unimodal distribution was observed (Fig. 5), showing that with respect to *l*/*h*, there were no distinct krill swarm types. Further, it is evident from the *l*/*h* distribution that the krill swarms were not spherical (i.e. spheres have *l*/*h*=1).

Krill swarms within the survey area exhibited a broad range of morphological variation, particularly in volume and area. Swarms generally were longer in the north-south direction, than east-west (Table 3), which may potentially be a consequence of current direction. On occasion, swarms filled up to 33% of the water column, but height and swarm minimum and maximum depths may otherwise have been constrained by water depth. The swarm energetic measures showed lower variation than morphological metrics, which may be biologically driven or a function of the sensitivity of the MBE (Table 3, coefficient of variation S_{v_mean} and S_{v_max}), or both. Swarm roughness (*R*=surface area/volume) had the lowest coefficient of variation (CV) for the morphological parameters, perhaps suggesting some underlying biological constraint (Cox et al., 2009).

The first three components of the PCA accounted for 22, 15 and 13%, respectively; of the observed variance in krill swarm structure (Table 3). The first principal component was influenced significantly by swarm volume, surface area, north-south length, east-west length and height. The second component was

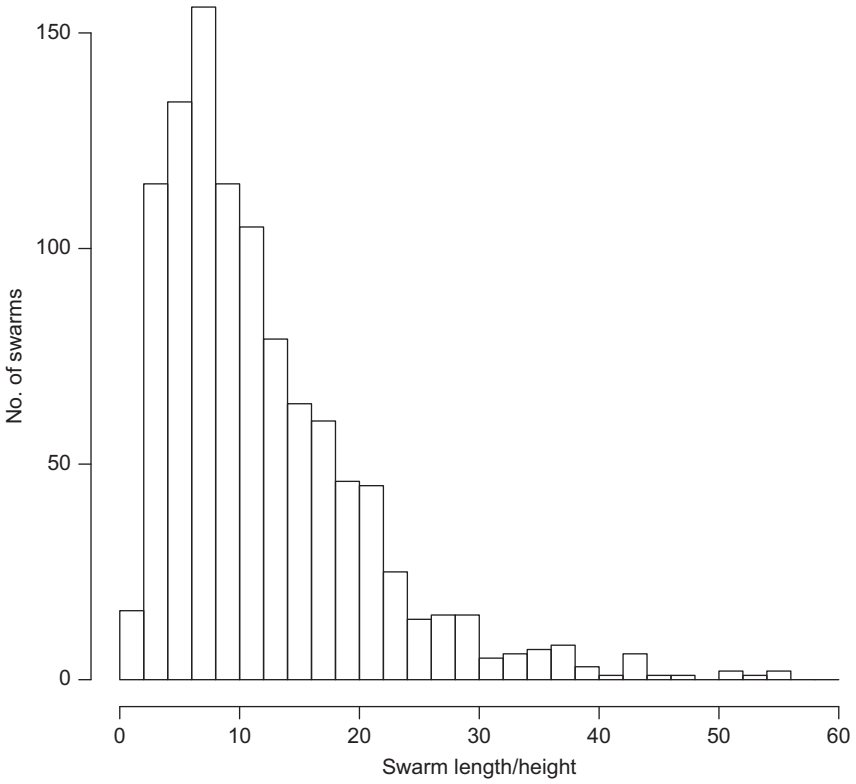

Fig. 5. Histogram of length/height ratio of 3-D detected krill swarms.

Table 3
Summary statistics for 3-D krill swarms for the 1006 swarms that were located entirely within the MBE swath during four days of surveying. CV is the coefficient of variation (CV=0.2 is 20%) and the first three principal components of krill swarm metrics. Principal component analysis was performed on the normalised correlation matrix of continuous krill swarm metrics. Swarm metrics with a significant influence on an individual principal component (j) are highlighted. Significant influence determined as eigenvector elements (u_{ij}) with $|u_{ij}| > 0.7.\max(|u_j|)$. $u_{ij} < 0.1$ are not shown.

Variable	Mean (CV)	Range	PC1	PC2	PC3
Variation explained (%)			22.4	14.8	13.4
Cumulative variation (%)			22.4	37.3	50.7
Mardias criterion			0.278	0.328	0.361
Roughness (m^{-1})	3.3 (0.23)	1.2 to 8.1	−0.115	−0.264	−0.106
Volume (m^3)	3695.7 (4.59)	46.2 to 406,709.8	**0.385**		0.28
Area (m^2)	11,024.7 (4.70)	218.6 to 1,222,048	**0.378**		0.278
North-south length (m)	120.2 (2.34)	9.9 to 4793.6	**0.384**	−0.271	−0.163
East-west length (m)	86.22 (2.03)	9.2 to 2959.5	**0.397**	−0.259	−0.14
Height (m)	10.6 (0.70)	3.9 to 77.5	**0.384**	0.147	0.217
Length/height	11.7 (1.34)	5.0 to 206.5	0.22	**−0.374**	−0.244
Latitude (deg)	−62.44	−62.46 to −62.41	0.127		**−0.403**
Longitude (deg)	−60.7	−60.77 to −60.66	−0.14	−0.18	**0.516**
Seabed depth (m)	94.6 (0.12)	45.3 to 134.2		−0.266	0.275
Position in water column	0.6 (0.32)	0 to 1	0.185	0.214	
S_{v_mean} (dB re 1 m^{-1})	−56.17 (0.14)	−99.77 to −44.75		**0.468**	
S_{v_min} (dB re 1 m^{-1})	−101.40 (14.75)	−108.03 to −51.62	−0.206	0.148	−0.123
S_{v_max} (dB re 1 m^{-1})	−51.04 (0.12)	−51.04 to −44.45	0.213	**0.393**	
Swarm nearest neighbour distance (m)	36.8 (0.93)	3 to 329.5		0.205	
Time of day (GMT)	16:35	12:58 to 22:10	0.122		−0.347
Cross-track distance (m)	27.1 (0.70)	0.9 to 94.0		−0.192	0.172

influenced significantly by the length to height ratio, and the third by geographical position and the swarm energetic parameters S_v and S_{v_max}.

No significant differences (at $p=0.05$) were found between the three-class cluster and other n-class clusters ($n=2$ to 10) using Beale's pseudo F-statistic test (Johnson, 1998) for significant differences in the residual sums of squares of the intra-cluster distances between two possible n-class swarm clusterings (e.g., a comparison between a 2-class clustering and the 3-class clustering).

The swarm partition analysis was carried out in the reduced factorial space determined by PCA. Swarm type one contained 158 swarms, and types two and three contained 431 and 417 swarms, respectively (Table 4). Swarm type three was the most distinct, exhibiting little overlap with the other types in principal

Table 4
Means of the three partition types for selected krill swarm metrics and associated coefficients of variation.

Swarm metric	Swarm type		
	1	2	3
Number of swarms	158	431	417
Roughness	3.23 (7.78)	2.96 (5.07)	3.65 (4.34)
Seabed depth (m)	88.02 (10.73)	90.82 (8.65)	101.00 (10.24)
S_v (dB re 1 m^{-1})	−51.89 (11.57)	−51.65 (7.75)	−57.44 (8.96)
Position in water column	0.78 (6.32)	0.73 (4.46)	0.55 (2.83)
Nearest-neighbour distance (m)	37.95 (1.39)	47.72 (1.11)	26.01 (1.16)
North-south length (m)	276.39 (0.41)	82.21 (1.17)	100.20 (2.06)
East-west length (m)	181.85 (0.43)	64.97 (1.22)	71.96 (2.02)
Height (m)	13.46 (1.21)	11.98 (1.57)	8.05 (2.24)
S_{v_min} (dB re 1 m^{-1})	−100	−99.51 (0.20)	−100 (0.09)
S_{v_max} (dB re 1 m^{-1})	−48.30 (11.88)	−48.32 (7.00)	−49.23 (13.75)
Cross-track distance (m)	33.87 (1.83)	29.80 (1.62)	40.42 (1.60)
Surface area (m^2)	29,197.01 (0.24)	11,554.54 (0.44)	3,591.56 (0.84)
Volume (m^3)	9237.07 (0.24)	4220.67 (0.43)	1053.37 (0.86)
Length/height	19.46 (0.54)	7.24 (1.67)	13.80 (1.83)
Swarm depth (m)	54.6 (0.32)	58.0 (0.32)	58.5 (0.29)
Seabed gradient	0.19 (0.46)	0.23 (0.89)	0.21 (0.36)

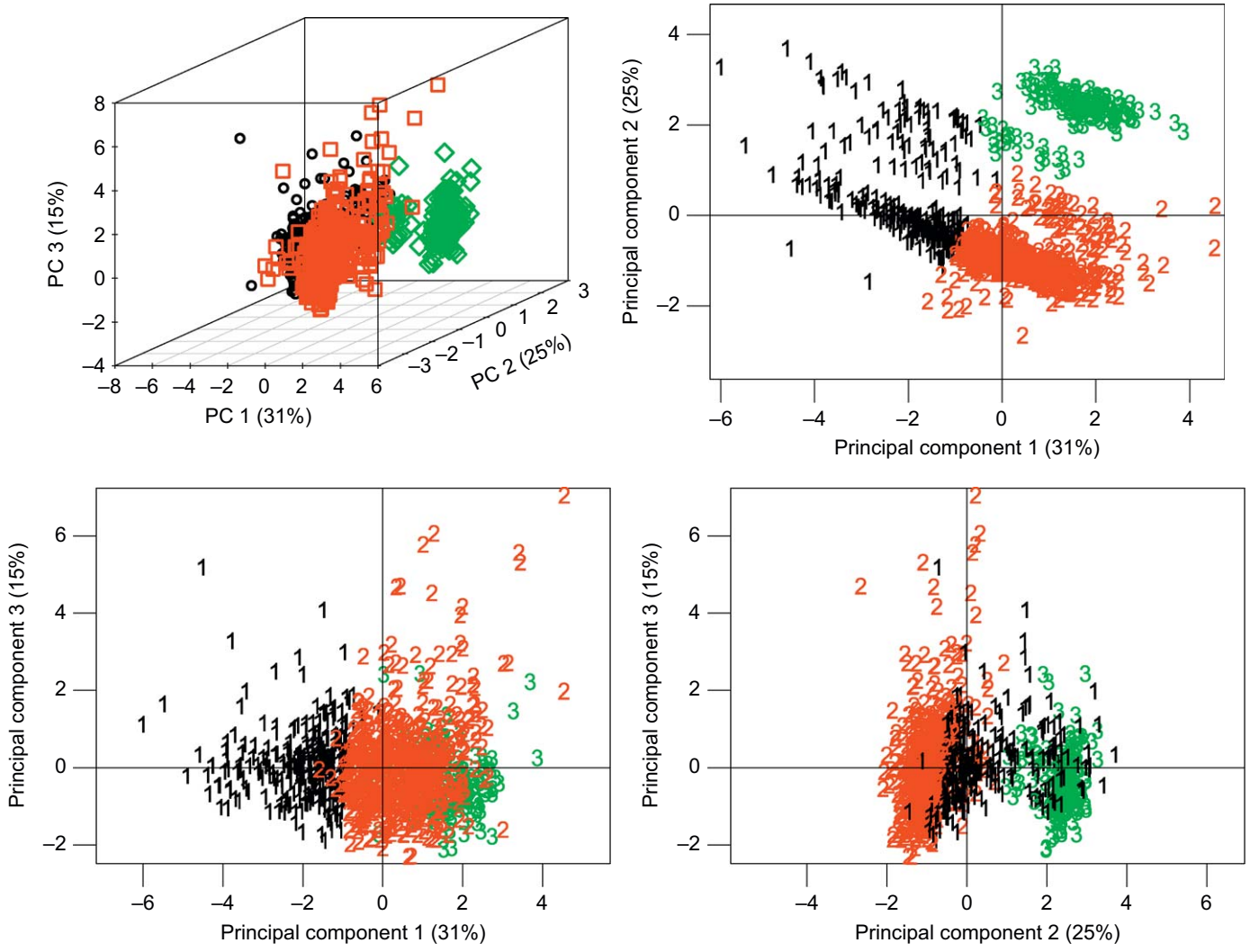

Fig. 6. Three-type partition analysis of krill swarms performed in principal component analysis reduced factorial space. The perceptive plot (top left) shows the first three principal components. Other panels show pairs of the first three principal components plotted on plane surfaces, illustrating changing overlap/separation between swarm types.

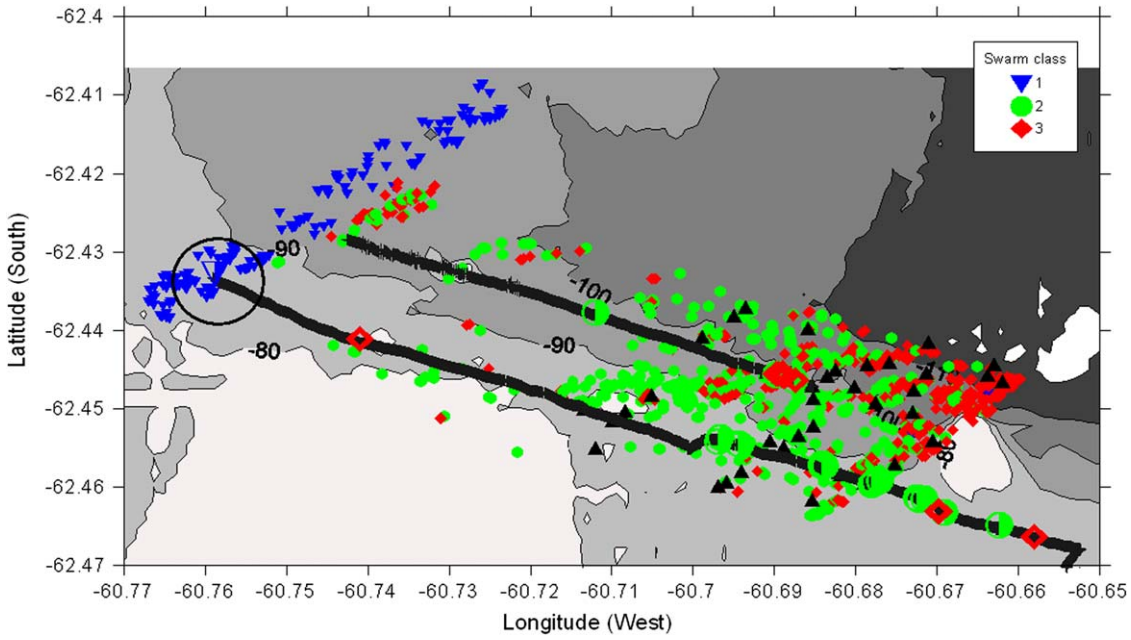

Fig. 7. The spatial distribution of krill-swarm types, sampled with a multi-beam echo sounder (MBE), classified using partition analysis. The seabed contours, given in 5-m intervals, were also derived from MBE observations. The positions of the two tie-lines are marked in black, with krill swarms detected while surveying along the tie-lines are shown as larger, half-filled symbols. Air-breathing krill-predator-encounter positions are given as solid black vertical triangles (Cox et al., 2009).

component planes 1 and 2, or planes 2 and 3 (Fig. 6). The other two swarm types showed increasing overlap, which is perhaps evidence that krill swarms were actually drawn from a continuum of swarm types, rather than a population of discrete swarm types.

Examining the geographic position of partitioned swarms revealed that type-one swarms were found entirely in the north-west of the survey area, whereas types two and three were found dispersed throughout the remainder of the site. A higher density of type-three swarms was found toward the east of the survey region, a region of particularly shallow water (depth=25 m, Fig. 7). Despite this cluster of type-three swarms in the shallow water area, seabed slope did not vary significant between the swarm types (Table 4). No air-breathing predators were observed in the region around the type-one krill swarms (Fig. 7).

While analysis of the *l*/*h* failed to separate krill swarms into distinct morphological types, there were distinct differences in this ratio across the three partitioned types: type-one had almost double the *l*/*h* ratio of type-three (Table 4). Swarms in type-one, while being smaller, exhibited a different morphological structure that was not simply rescaled for larger swarm sizes. For example, the north-south and east-west lengths of type one swarms were more than double that of types-two and three, but heights were not doubled between swarm types. This suggests that swarm types are not simply driven by rescaling of a 'standard' swarm.

4. Discussion

This investigation has shown that MBE (200 kHz Simrad-Mesotech SM20) is capable of detecting Antarctic krill swarms, and that small boats are suitable platforms for conducting acoustic surveys in areas inaccessible to ocean-going research vessels. Further application of MBE technology deployed from a variety of platforms – e.g., boats, moorings, and autonomous underwater vehicles (AUVs) – has the potential to contribute much to krill research (Nicol and Brierley, 2010). Using the MBE, we found that krill swarms formed complex 3-D shapes, which were spatially segregated, and that, potentially, the nearshore waters of the South Shetlands contain a large biomass of krill.

Our analyses were based on an objectively-defined krill swarm boundary, identified using a 3-D detection algorithm, with parameters selected by sensitivity analysis (Table 2). Previous researchers have used automated ping-by-ping image recognition software to delineate pelagic aggregations observed by omni-directional MBEs in 3-D (e.g., Misund et al., 1998; Brehmer et al., 2006). It is our understanding, however, that this investigation is the first MBE study that has assessed the influence of the parameters used in an automatic 3-D detection algorithm on the resultant aggregation metrics.

Previously, researchers have used single aggregation metrics, or ratios of aggregation metrics to describe aggregation type. For example, Gerlotto et al. (2004) acquired 3-D data from aggregations of anchovy (*Engraulis ringens*) and common sardine (*Strangomera bentincki*) using an MBE, and suggested that layers and schools could be partitioned by an aggregation length-to-height ratio of *l*/*h*=7. No such break point occurred in the observed *l*/*h* ratios of the krill swarms detected in this investigation (Fig. 6). Rather, the MBE results suggest a continuum of swarm *l*/*h*: the use of single swarm metrics or metric ratios are not useful discriminators for the krill swarms observed during this investigation. Consequently, multivariate analysis techniques were employed.

The results of the multivariate analysis techniques employed during this research (Tables 3 and 4, Fig. 7) demonstrated that groups may occupy different geographical areas (Fig. 7), and that spatial segregation between groups can occur over small distances (ca. 3 km) and have sharp boundaries (Fig. 7). Through the use of two tie lines, surveyed perpendicularly to the main survey lines (Fig. 1 and Fig. 7), that cut through the south-east and north-west areas of the study site, we have been able to discount a day affect in our observations. If swarm segregation was simply caused by a day affect, then type-one swarms would have been detected in the eastern end of the survey site and types-two and three in the western area of the

survey site. However, only one swarm was detected in the western area along a tie line, and this was a type-one swarm providing strong evidence that the swarm type segregation was truly spatial and not a day affect (Fig. 7). The temporal persistence of swarm type, elucidated by data collected along the surveyed tie lines, suggests that the causes of swarm-type segregation may be spatially persistent, such as water depth or prevailing water current.

We cannot be certain of the causes of the spatial persistence of krill swarms observed during this investigation. The next step would be to sample the physical environment and to make targeted trawls through individual krill swarms to examine possible relationships between swarm metrics and characteristics of krill within swarms such as length-distribution, stage, and sex ratio. This would enable assessment of the role of swarm size-sorting mechanisms, as suggested by Watkins et al. (1992) and previously observed on the west of the Antarctic Peninsula by Lascara et al. (1999).

The spatial segregation of krill-swarm types in nearshore areas may be of significance for land-based, air-breathing krill predators that have constrained foraging-trip durations during the breeding season. Should swarms of different types be comprised of krill that are of different sizes, then the predators may gain energetic benefits from focussing foraging effort on particular swarm types. Conversely, escape responses of individual krill in a swarm may also vary by swarm type: naïve individuals in a swarm may have ineffective escape response (O'Brien, 1989; Ritz, 1994). The potential differences in krill escape response, coupled with the swarm spatial segregation observed during this study (Fig. 7), suggest that krill catchability by predators may vary considerably at small scales (ca. 3 km), and may explain why no air-breathing predators were observed foraging in the vicinity of type-one swarms (Fig. 7).

The 3-D classification of krill swarm type may in the future assist in the partitioning of acoustic echoes to separate those arising from krill swarms and those from other species. Such an analysis was carried out by Woodd-Walker et al. (2003) using 2-D observations of krill swarms from conventional, vertically downward-oriented, single-beam echo-sounders. However, problems with the classification of acoustic targets remain. Fielding et al. (2007) suggested that Mackerel icefish (*Champsocephalus gunnari*) have been incorrectly acoustically classified as Antarctic krill using a two-frequency dB-difference technique (Brierley et al., 1998), thus positively biasing krill areal density estimates, $\hat{\rho}$. Considering 3-D krill-swarm metrics, rather than just a conventional two-frequency dB-difference technique, may enable the acoustic echoes from mackerel icefish to be eliminated from $\hat{\rho}$, thus reducing the positive bias that arises from incorrect identification of acoustic echoes.

This research has demonstrated the krill can be detected with MBEs, and that the data are useful for ecological studies, e.g., determining the spatial segregation of swarm types. Considerable work is still required before MBE data can be used for directly calculating $\hat{\rho}$, such as in devising field-calibration procedures. Fortunately, some progress is being made with: MBE calibration procedures (e.g., Foote et al., 2005); estimating krill target strength at any insonified angle (e.g., Demer and Conti, 2005); and accounting for the directivity of krill scatter perceived by an MBE (e.g., Cutter et al., 2009). Even now, however, 3-D swarm type information derived from MBE observations may enable researchers to improve identification of krill swarms and exclude other species from biomass estimates, thereby reducing bias. MBEs provide a wider-eyed view of the world of krill, and we expect MBEs to add much to our understanding of this key Antarctic species.

Acknowledgments

We thank the Royal Society for funds enabling deployment of the MBE, and Jeff Condiotty of Simrad USA for the loan of the SM20. We are grateful to Rennie Holt, Director of the United States Antarctic Marine Living Resources program, for availing numerous resources and providing both financial and logistical support. We thank the Master, officers and crew of the R/V *Yuzhmorgeologiya*, and the personnel at the Cape Shirreff field station for logistical support. MJC was supported by a UK Natural Environment Research Council CASE PhD studentship. This work was conducted as a complement to JDW's and DAD's NSF-funded investigation of the Livingston Island nearshore environment (Grant #06-OPP-33939). We thank A. Jenkins and M. Van Den Berg for skippering the nearshore boats and S. Sessions for skippering the nearshore boats and providing invaluable field expertise.

References

Alonzo, S.H., Mangel, M., 2001. Survival strategies and growth of krill: avoiding predators in space and time. Marine Ecology Progress Series 209, 203–217.

Barange, M., Miller, D.G.M., Hampton, I., Dunne, T.T., 1993. Internal structure of Antarctic krill (*Euphausia superba*) swarms based on acoustic observations. Marine Ecology Progress Series 99, 205–213.

Barange, M., 1994. Acoustic identification, classification and structure of biological patchiness on the edge of the Agulhas Bank and its relation to frontal features. South African Journal of Marine Science 14, 333–347.

Brehmer, P., Lafont, T., Georgakerakos, S., Josse, E., Gerlotto, F., Collet, C., 2006. Omnidirectional multibeam sonar monitoring: applications in fisheries science. Fish and Fisheries 7, 165–179.

Brierley, A.S., Ward, P., Watkins, J.L., Goss, C., 1998. Acoustic discrimination of Southern Ocean zooplankton. Deep-Sea Research II 45, 1155–1173.

Coetzee, J., 2000. Use of a shoal analysis and patch estimation system (SHAPES) to characterise sardine schools. Aquatic Living Resources 13 (1), 1–10.

Cox, M.J., Demer, D.A., Warren, J.D., Cutter, G.R., Brierley, A.S., 2009. Multibeam echosounder observations of swarms of Antarctic krill (*Euphausia superba*) provide new insight to interactions between krill and air breathing predators. Marine Ecology Progress Series 378, 199–209.

Cutter, G.R., Renfree, J.S., Cox, M.J., Brierley, A.S., Demer, D.A., 2009. Modelling three-dimensional directivity of sound scattering by Antarctic krill: progress towards biomass estimation using multibeam sonar. ICES Journal of Marine Science 66 (6), 1245–1251.

Demer, D.A., Conti, S.G., 2005. New target-strength model indicates more krill in the Southern Ocean. ICES Journal of Marine Science 62, 25–32.

Everson, I., Miller, D.G.M., 1994. Krill mesoscale distribution and abundance: results and implications of research during the BIOMASS Programme. In: E1-Sayed, S.Z. (Ed.), Southern Ocean Ecology: The BIOMASS Perspective. Cambridge University Press, Cambridge, pp. 129–143.

Foote, K.G., Knudsen, H.P., Vestnes, G., MacLennan, D.N., Simmonds, E.J., 1987. Calibration of acoustic instruments for fish density estimation: a practical guide. ICES Cooperative Research Report 144, 57.

Foote, K.G., Chu, D., Hammar, T.R., Baldwin, K.C., Mayer, L.A., Hufnagle Jr., L.C., Jech, M.J., 2005. Protocols for calibrating multibeam sonar. Journal of the Acoustical Society of America 117 (4), 2013–2027.

Fielding, S., Collins, M., Everson, I., Reid, A., 2007. Improving target identification of mackerel icefish using commercial and scientific acoustic observations. Report to the ICES Working Group on Fisheries Acoustics, Science and Technology (WGFAST), Dublin, Ireland.

Genin, A., 2004. Bio-physical coupling of the formation of zooplankton and fish aggregations over abrupt topographies. Journal of Marine Systems 50, 3–20.

Gerlotto, F., Soria, M., Freon, P., 1999. From two dimensions to three: the use of multibeam sonar for a new approach in fisheries acoustics. Canadian Journal of Fisheries and Aquatic Science 56, 6–12.

Gerlotto, F., Castillo, J., Saavedra, A., Barbieri, M.A., Espejo, M., Cotel, P., 2004. Three-dimensional structure and avoidance behaviour or anchovy and common sardine schools in central Chile. ICES Journal of Marine Science 61, 1120–1126.

Hamner, W.M., Hamner, P.P., 2000. Behavior of Antarctic krill (*Euphausia superba*): schooling, foraging, and antipredatory behavior. Canadian Journal of Fisheries and Aquatic Sciences 57, 192–202.

Hewitt, R.P., Demer, D.A., 2000. The use of acoustic sampling to estimate the dispersion and abundance of euphausiids, with an emphasis on Antarctic krill *Euphausia Superba*. Fisheries Research 47, 215–229.

Hofmann, E.E., Haskell, A.G.E., Klinck, J.M., Lascara, C.M., 2004. Lagrangian modelling studies of Antarctic krill (*Euphausia superba*) swarm formation. ICES Journal of Marine Science 61, 617–631.

Johnson, D.E., 1998. In: Applied Multivariate Methods for Data Analysis. Duxbury Press, California, USA.

Lascara, C.M., Hofmann, E.E., Ross, R.M., Quetin, L.B., 1999. Seasonal variability in the distribution of Antarctic krill, Euphausia superba, west of the Antarctic Peninsula. Deep-Sea Research I 46, 951–984.

Mardia, K.V., Kent, J.T., Bibby, J.M., 1979. Multivariate Analysis. Probability and Mathematical Statistics. Academic Press, London.

Mauchline, J., 1980. Studies on patches of krill, *Euphausia superba* Dana. BIOMASS Handbook No. 6.

Melvin, G.D., Cochrane, N.A., Yanchao, L., 2003. Extraction and comparison of acoustic backscatter from a calibrated multi- and single-beam sonar. ICES Journal of Marine Science 60, 669–677.

Miller, D.G.M., Hampton, I., 1989. Biology and ecology of the Antarctic krill (*Euphausia superba* Dana): a review. BIOMASS Science Series No. 9.

Miller, D.G.M., Barange, M., Klindt, H., Murray, A.W.A, Hampton, I., Siegel, V., 1993. Antarctic krill aggregation characteristics from acoustic observations in the Southwest Atlantic Ocean. Marine Biology 117, 171–183.

Misund, O.A., Ferno, A., Pitcher, T., Totland, B., 1998. Tracking herring schools with a high resolution sonar. Variations in horizontal area and relative echo intensity. ICES Journal of Marine Science 55, 58–66.

Murphy, E.J., Morris, D.J., Watkins, J.L., Priddle, J., 1988. Scales of interactions between Antarctic krill and the environment, Antarctic Ocean and Re-sources Variability. Springer-Verlag, Berlin, Germany, pp. 120–130.

Nicol, S., Brierley, A.S., 2010. Through a glass less darkly—new approaches for studying the distribution, abundance and biology of Euphausiids. Deep-Sea Research II 57 (7–8), 496–507.

O'Brien, D.P., 1987. Description of escape responses of krill (Crustacea: Eupausiacea), with particular reference to swarming behaviour and the size and proximity of the predator. Journal of Crustacean Biology 7 (3), 449–457.

O'Brien, D.P., 1989. Analysis of the internal arrangement of individuals within crustacean aggregations (Eupausiacea, Mysidacea). Journal of Experimental Marine Biology and Ecology 128, 1–30.

Reid, D.G., Simmonds, E.J., 1993. Image analysis techniques for the study of fish school structure from acoustic survey data. Canadian Journal of Fisheries and Aquatic Science 50, 886–893.

Ritz, D.A., 1994. Social aggregation in pelagic invertebrates. Advances in Marine Biology 30, 155–216.

Ritz, D.A., 2000. Is social aggregation in aquatic crustaceans a strategy to conserve energy? Canadian Journal of Fisheries and Aquatic Sciences 57 (S3), 56–67.

Simmonds, J.E., MacLennan, D.N., 2005. Fisheries Acoustics. Chapman & Hall, London.

Szulkin, M., Dawidowicz, P., Dodson, S.I., 2006. Behavioural uniformity as a response to cues of predation risk. Animal Behaviour 71, 1013–1019.

Tarling, G.A., Roudy-Cuzin, J., Thorpe, S.E., Shreeve, R.S., Ward, P., Murphy, E.J., 2007. Recruitment of Antarctic krill *Euphausia superba* in the South Georgia region: adult fecundity and the fate of larvae. Marine Ecology Progress Series 331, 161–179.

Trathan, P.N., Brierley, A.S., Brandon, M.A., et al., 2003. Oceanographic variability and changes in Antarctic krill (*Euphausia superba*) abundance at South Georgia. Fisheries Oceanography 12 (6), 569–583.

Watkins, J.L., Morris, D.J., Ricketts, C., Priddle, J., 1986. Difference between swarms of Antarctic krill and some implications for sampling krill populations. Marine Biology 93, 137–146.

Watkins, J.L., Buchholz, F., Priddle, J., Morris, D.J., Ricketts, C., 1992. Variation in reproductive status of Antarctic krill swarms; evidence of size-related sorting mechanism? Marine Ecology Progress Series 82, 163–174.

Watkins, J.L., Murray, A.W.A., 1998. Layers of Antarctic krill, *Euphausia superba*: are they just long krill swarms? Marine Biology 131, 237–247.

Woodd-Walker, R.S., Watkins, J., Brierley, A.S., 2003. Identification of Southern Ocean acoustic targets using aggregation backscatter and shape characteristics. ICES Journal of Marine Science 60, 641–649.

Zamon, J.E., Greene, C.H., Eli, M.T., Demer, D.A., Hewitt, R.P., Sexton, S., 1996. Acoustic characterization of the three-dimensional prey field of foraging Chinstrap Penguins. Marine Ecology Progress Series 131, 1–10.